

Saturation-Aware Model Predictive Energy Management for Droop-Controlled Islanded Microgrids*

Steffen Hofmann¹, Ajay Sampathirao¹, Christian A. Hans¹, Jörg Raisch¹, Alexander Heidt² and Erich Bosch²

Abstract—In this paper, we propose a minimax model predictive control (MPC)-based energy management system that is robust with respect to uncertainties in renewable infeed and load. The MPC formulation includes a model of low-level droop control with saturation at the power and energy limits of the units. Robust MPC-based energy management systems tend to under-utilize the renewable energy sources to guarantee safe operation. In order to mitigate this effect, we further consider droop control of renewable energy sources.

For a microgrid with droop-controlled units, we show that enhancing droop feedback with saturation enlarges the space of feasible control actions. However, the resulting controller requires to solve a mixed-integer problem with additional variables and equations representing saturation. We derive a computationally tractable formulation for this problem. Furthermore, we investigate the performance gained by using droop with saturation, renewable droop and combination of both in a case study.

Index Terms—Robust model predictive control, Energy management system, Saturation, Droop control, Microgrid.

I. INTRODUCTION

Decarbonization of the energy sector is promoting a worldwide increase in the deployment of renewable energy [1]. This shifts the foundation of power systems from large, centralized generation units to smaller distributed energy resources (DERs). However, the volatility associated with renewable generation has posed serious challenges for their integration into the existing power system setups. In this context, the microgrid (MG) concept represents a promising direction [2]. In [3], an MG is defined as follows: “Generally, a microgrid is defined as a group of DERs, including Renewable Energy Resources (RES) and Energy Storage Systems (ESS), and loads, that operate together locally as a single controllable entity. Microgrids exist in various sizes and configurations; they can be large and complex networks with various generation resources and storage units serving multiple loads, or small and simple systems supplying a single customer.”

Here, we focus on islanded operation of MGs. In such an MG, the energy management system (EMS) is responsible for deciding the power set-points of the generation units to meet the demand locally and ensure an economic operation. Usually, the EMS provides the power set-points on a time scale ranging between minutes to fraction of an hour, guaranteeing safe operation without violation of power and energy limits of the units. On the lower control layers, often droop-based

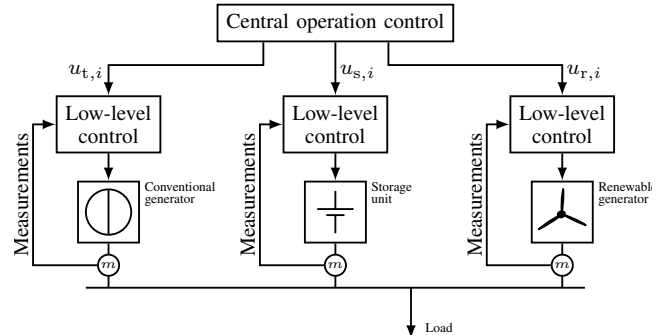


Figure 1. Block diagram representation: the central operation control provides power set-points to the units; the units change their power output based on a primary control law to ensure a power balance. The primary control laws of the different units can have saturation according to operation limits.

control strategies are used to maintain power balance (see, e. g., [4]). This is shown in Figure 1.

Various control strategies to design EMSs are available in literature. Some of these strategies are reviewed in [5]. One popular strategy presented there is model predictive control (MPC), which is a finite-horizon optimal control strategy that determines the control actions (e. g., power set-points) by solving an optimization problem. At each time instance, an optimization problem is formulated based on renewable infeed forecast, demand forecast and the current state of the MG and solved. From the resulting sequence of control actions, only the first control action is applied to the system. At the next time instance, the optimization problem is updated with the new state and forecasts and solved again. A valuable feature of this control technique is its ability to account for constraints such as power and energy limits. MPC-based EMSs are designed, e. g., in [6], [7].

Fluctuations in renewable infeed and load demand can compromise safe and reliable operation of MGs. In literature there are MPC designs that are capable of handling uncertainty (see, e. g., [8], [9], [10]). In [7], the authors propose a minimax (MM) MPC approach to address the uncertain load and renewable infeed. This design considers the impact of droop control on the operation.

As opposed to an MPC-EMS approach, pure droop schemes aiming for economic objectives are proposed in [11], [12], [13]. In [11], a non-linear droop control law that prioritizes generation from units with less operation cost is suggested. Furthermore, a strategy for tuning the droop gradient in accordance with the generation cost is proposed in [12]. In [13], a linear droop scheme based on incremental cost of power generation is considered. In [14], it is stated that when the operation costs are strictly convex, selecting a suitable droop

¹Technische Universität Berlin, Control Systems Group, Germany, {hofmann, sampathirao, hans, raisch}@control.tu-berlin.de.

²Autarsys GmbH, Berlin, Germany, {heidt, bosch}@autarsys.com.

*This work was supported by the German Federal Ministry for Economic Affairs and Energy (BMWi), Project No. 0324024A.

control law can lead to an economic operation. One limitation of these approaches is their omission of storage dynamics and energy limits. Also, it is not possible to consider turning on and off the conventional generators.

A major drawback of the MM MPC proposed in [7] is its conservativeness: the power and energy limits are included as constraints and the power set-points are selected such that purely affine droop feedback would not violate these constraints for all possible disturbance realizations. Thereby, this approach avoids saturation in the local unit controllers. The limitation of avoiding actuator saturation in MPC designs is recognized in [15], [16], [17]. These works provide theoretical results to include this effect in feedback control of MM MPC. However, the proposed approaches are not directly applicable to MGs. For instance, they do not include binary decision variables that result from switching on and off conventional units and, in contrast to our MG system, assume state feedback control.

Another limitation of most of the aforementioned power system control designs is their exclusion of renewable energy systems (RES) in droop control. These designs consider droop control only for storage and conventional units. Increasing penetration of RES has encouraged developing droop strategies for RES (see, e.g., [18], [19], [20], [21]). They can increase the energy generated from renewable units, especially during periods with sufficient availability. The benefit of droop control for renewable units in the reliable operation of a grid-connected MG without energy storage is demonstrated in [21]. Similar results, including a practical study, are shown for an islanded scenario in [20]. Such works encouraged us to extend the previous MM EMS design (see [7]) for systems with RES droop, expecting an improvement in the overall performance.

A. Contributions

The main contributions of this paper are as follows.

- 1) We propose an MM MPC-based EMS that is both economic and robust. As compared to a related existing solution [7], we improve performance by including RES droop and droop saturation.
- 2) The MM MPC with saturation corresponds to a robust mixed-integer program. Existing tractable reformulations (see, e.g., [22]) are not directly applicable as the droop control with saturation constitutes a piecewise affine function. We derive a tractable reformulation of the MM MPC problem considered here.
- 3) We show that the proposed controller increases the feasible set of controls over MM MPC without saturation.
- 4) In a case study, we demonstrate performance improvement resulting from saturation and RES droop in terms of open-loop predicted cost as well as closed-loop cost.

B. Structure of the paper

The structure of this paper is as follows. Section II provides the mathematical model of an islanded MG, droop control and saturation. Section III defines the control objective and two MM MPC problems - one with RES droop and one with RES droop and saturation in all the units. In Section IV, we present

a tractable reformulation of the MM MPC problem and also prove the increase of the feasible region. Section V provides a case study comparing MM MPC controllers with and without saturation and with and without RES droop control.

C. Mathematical preliminaries

The set of real numbers is denoted by \mathbb{R} . The sets of negative, positive, non-positive and non-negative real numbers are denoted by $\mathbb{R}_{<0}$, $\mathbb{R}_{>0}$, $\mathbb{R}_{\leq 0}$ and $\mathbb{R}_{\geq 0}$, respectively. The set of positive integers is denoted by \mathbb{N} , and $\mathbb{N}_{[1,n]} = \{1, 2, \dots, n\}$ is the set of the first n positive integers.

The operator $\min(x, y)$ provides the element-wise minimum of the vectors x, y . Similarly, $\max(x, y)$ provides the element-wise maximum. If x and y are vectors or matrices of equal dimensions, then a comparison such as $x \leq y$ is true if and only if (iff) all comparisons between elements at matching positions are true. If x is a matrix and y is a vector, then a comparison is true iff comparing every column in x to y according to the previous sentence evaluates to true. If x is a vector or matrix and y is a scalar, then a comparison is true iff comparing every single element in x to y evaluates to true. If x and y are vectors or matrices of equal dimensions and $x \leq y$, then the set $[x, y]$ is the box determined by the intervals defined by elements at matching positions.

For a vector or matrix x , the transpose is denoted by x^T . For a vector $x \in \mathbb{R}^n$ with elements x_i , we use the notation $\mathbf{1}^T x = \sum_{i=1}^n x_i$. For $x \in \mathbb{R}$ and $\delta \in \{0, 1\}$, we define $y = \delta \wedge x$ as: $y = x$ if $\delta = 1$ and $y = 0$ if $\delta = 0$. When x and δ are vectors, this operation is performed element-wise. We sometimes use a dot to indicate that function arguments are omitted for brevity, e.g., writing $x(\cdot, \rho)$.

We explicitly point out that when we classify a function as *increasing* or *monotonically increasing*, respectively *decreasing* or *monotonically decreasing*, we allow it to be constant or constant in parts; i.e., we do *not* imply *strict* monotonicity.

II. MIROGRID MODEL

In this section, we develop the mathematical model of an islanded MG including droop control and saturation limits. The model of the MG and the notation are motivated from [7], [23] and related works. This model is used later for the EMS design.

For the model, we assume that the lower control layers (also referred to as low-level control in this paper), i.e., primary and secondary control ensure a stable operation of the MG. In addition, we assume that start-up and shut-down times of the conventional units are small compared to the EMS sampling time. Furthermore, we assume that storage losses are negligible compared to the uncertainties posed by the RES and load demand.

A. Notation

We consider the MG model with RES like wind turbines and photovoltaic (PV) plants, battery storage units and conventional units like diesel generators. Each unit in the MG is provided with a power set-point from the EMS. However, the

uncertainty both in generation from the RES and in demand necessitates power outputs that differ from these set-points.

In the MG, let us denote the number of conventional units, storage units and renewable units by T , S and R , respectively, and the number of loads by D . At a given sampling instance $k \in \mathbb{N}_{\geq 0}$, let us denote the disturbance by $w(k) = [w_r(k)^\top w_d(k)^\top]^\top$, where $w_r(k) \in \mathbb{R}_{\geq 0}^R$ is the available renewable infeed and $w_d(k) \in \mathbb{R}_{\leq 0}^D$ is the load demand. The power set-points provided by the EMS are denoted by $u(k) = [u_t(k)^\top u_s(k)^\top u_r(k)^\top]^\top$, where $u_t(k) \in \mathbb{R}^T$, $u_s(k) \in \mathbb{R}^S$ and $u_r(k) \in \mathbb{R}^R$ are the set-points of the conventional units, storage units and RES, respectively. Each conventional unit can be switched on or off, which is represented by a vector of binary variables $\delta_t(k) \in \{0, 1\}^T$. The power output of the units is denoted by $p(k) = [p_t(k)^\top p_s(k)^\top p_r(k)^\top]^\top$, where $p_t(k) \in \mathbb{R}_{\geq 0}^T$, $p_s(k) \in \mathbb{R}^S$ and $p_r(k) \in \mathbb{R}_{\geq 0}^R$. The energy level of storage units is denoted by $x(k) \in \mathbb{R}_{\geq 0}^S$.

B. Microgrid without saturation and without renewable power sharing

In an islanded MG, the local generation should match the local consumption at all time instances. This power balance condition can be represented by the algebraic equation

$$\mathbf{1}^\top p_t(k) + \mathbf{1}^\top p_s(k) + \mathbf{1}^\top p_r(k) + \mathbf{1}^\top w_d(k) = 0. \quad (1)$$

The power provided by the renewable units depends on the available renewable infeed $w_r(k)$ and the power set-points $u_r(k)$, i. e.,

$$p_r(k) = \min(u_r(k), w_r(k)). \quad (2)$$

The uncertain load $w_d(k)$ and renewable infeed $p_r(k)$ cause mismatch in the power balance. This mismatch is compensated by the storage and conventional units [4]. Each unit has a low-level droop control that ensures a desired proportional power sharing (see, e. g., [24], [25]). The share of each unit depends on the inverse droop gain, which we denote by $\chi_t \in \mathbb{R}_{\geq 0}^T$ for the conventional units and $\chi_s \in \mathbb{R}_{\geq 0}^S$ for the storage units. These inverse droop gains can be chosen, e. g., according to the nominal power of the units. Let us denote $\chi = [\chi_t^\top \chi_s^\top]^\top$.

Consider an auxiliary free variable $\rho(k) \in \mathbb{R}$. In steady-state, the power of the storage units can be described by

$$p_s(k) = u_s(k) + \chi_s \rho(k). \quad (3a)$$

The dynamics of the storage units are

$$x(k) = x(k-1) - T_s p_s(k), \quad (3b)$$

where $T_s \in \mathbb{R}_{> 0}$ is the sampling time. The energy storage capacities are included by the constraints

$$x^{\min} \leq x(k) \leq x^{\max}, \quad (3c)$$

with $x^{\min} \in \mathbb{R}_{\geq 0}^S$ and $x^{\max} \in \mathbb{R}_{> 0}^S$.

Conventional units can be switched on or off. When conventional unit $i \in \mathbb{N}_{[1, T]}$ is switched off, i. e., $\delta_{t,i}(k) = 0$, then its power $p_{t,i}(k) = 0$ and it cannot participate in power sharing. When switched on, i. e., $\delta_{t,i}(k) = 1$, it participates in power sharing. This behavior can be modeled by

$$p_t(k) = \delta_t(k) \wedge (u_t(k) + \chi_t \rho(k)). \quad (4)$$

The constraints on the power set-points and the power of the units are

$$u^{\min} \leq u(k) \leq u^{\max}, \quad (5a)$$

$$\begin{bmatrix} \delta_t(k) \wedge p_t^{\min} \\ p_s^{\min} \\ p_r^{\min} \end{bmatrix} \leq p(k) \leq p^{\max}, \quad (5b)$$

with $u^{\min} \in \mathbb{R}^{T+S+R}$, $u^{\max} \in \mathbb{R}^{T+S+R}$, $p^{\min} \in \mathbb{R}_{\geq 0}^T \times \mathbb{R}_{< 0}^S \times \mathbb{R}_{\geq 0}^R$ and $p^{\max} \in \mathbb{R}_{> 0}^{T+S+R}$. We subdivide these limits in the same manner as $u(k)$ and $p(k)$, e. g., $p^{\min} = [(p_t^{\min})^\top (p_s^{\min})^\top (p_r^{\min})^\top]^\top$.

C. Microgrid with renewable power sharing

In the previous model, we have restricted power sharing to storage and conventional units. However, as we already considered the limitation due to available renewable power, we can also include renewable units in power sharing. Let us define $\chi_r \in \mathbb{R}_{\geq 0}^R$ and redefine the vector of inverse droop constants by $\chi = [\chi_t^\top \chi_s^\top \chi_r^\top]^\top$. Then the renewable power (2) is redefined as

$$p_r(k) = \min(u_r(k) + \chi_r \rho(k), w_r(k)). \quad (6)$$

D. Microgrid with saturation

We consider saturation as a hard limiter enforcing the physical operation range of a unit. Therefore, the power output of units with droop control given by (3a), (4), (6) is now expressed as a feedback law of $\rho(k)$ and saturation. Let us define saturation of a variable (for example, p) as

$$\text{sat}(p^{\min}, p, p^{\max}) := \begin{cases} p^{\min}, & \text{if } p < p^{\min}, \\ p, & \text{if } p \in [p^{\min}, p^{\max}], \\ p^{\max}, & \text{if } p > p^{\max}, \end{cases} \quad (7)$$

where $p^{\min} \leq p^{\max}$. When p , p^{\min} and p^{\max} are vectors, the $\text{sat}(\cdot, \cdot, \cdot)$ operator is understood element-wise.

With saturation, operation constraints are imposed by limiting the output power at the lower control layer. Now the renewable power (6) is redefined as

$$p_r(k) = \text{sat}(p_r^{\min}, u_r(k) + \chi_r \rho(k), w_r(k)). \quad (8)$$

Note that (6) already includes saturation at the upper limit.

For conventional generators, the power given by (4) is redefined as

$$p_t(k) = \delta_t(k) \wedge \text{sat}(p_t^{\min}, u_t(k) + \chi_t \rho(k), p_t^{\max}). \quad (9)$$

Operation of storage units is restricted by power as well as energy limits. A straightforward way to implement energy-based saturation would involve setting the power to zero in the moment the energy reaches one of the bounds in (3c). However, to avoid such sudden power changes, which could happen also between sampling instances of the EMS, and to keep the analysis simple, we choose a different approach.

Based on the sampling time T_s and current energy level x , dynamically adjusted power limits are determined by

$$\begin{aligned} \bar{p}_s^{\min}(k) &= \max\left(p_s^{\min}, \frac{x(k-1) - x^{\max}}{T_s}\right), \\ \bar{p}_s^{\max}(k) &= \min\left(p_s^{\max}, \frac{x(k-1) - x^{\min}}{T_s}\right), \end{aligned} \quad (10a)$$

and the power is subject to saturation at these limits, i. e.,

$$p_s(k) = \text{sat}(\bar{p}_s^{\min}(k), u_s(k) + \chi_s \rho(k), \bar{p}_s^{\max}(k)). \quad (10b)$$

Remark 1: When the power sharing constant of a unit is $\chi_i = 0$, for $i \in \mathbb{N}_{[1, T+S+R]}$, then the unit does not participate in power sharing. This means flexibility to decide which units can participate in power sharing.

Remark 2: Please note that in the saturation-based model, the power set-point limits u^{\min} and u^{\max} in (5a) can differ from and even lie beyond the power limits p^{\min} and p^{\max} .

Remark 3: Also note that now the explicit energy and power constraints (3c) and (5b) are no longer required. Instead, the limits x^{\min} , x^{\max} , p^{\min} and p^{\max} are implicitly enforced by saturation.

III. MINIMAX MPC FOR MICROGRID WITH SATURATION

The goal is to design an MPC-based EMS that is robust w. r. t. uncertain available renewable infeed and load demand. We consider an MM formulation where the worst-case operation cost of the MG over all possible disturbance realizations is minimized [9]. In this section, we define the uncertainty, the operation cost and later formulate the MM MPC problem.

A. Uncertainty model

For the considered renewable units, the available power depends on the weather conditions (i. e., solar irradiation for PV plants and wind speed for wind turbines). Using historic data and a forecaster, future lower and upper bounds for the available power can be derived (see, e. g., [26]). Let us denote these bounds at time instance k by

$$w_r^{\min}(k) \leq w_r(k) \leq w_r^{\max}(k), \quad (11)$$

where $w_r^{\min}(k) \in \mathbb{R}_{\geq 0}^R$ and $w_r^{\max}(k) \in \mathbb{R}_{\geq 0}^R$. Similarly, the minimum and maximum bounds for the load demands are

$$w_d^{\min}(k) \leq w_d(k) \leq w_d^{\max}(k), \quad (12)$$

where $w_d^{\min}(k) \in \mathbb{R}_{\leq 0}^D$ and $w_d^{\max}(k) \in \mathbb{R}_{\leq 0}^D$. Based on (11), (12) we can pose

$$w^{\min}(k) \leq w(k) \leq w^{\max}(k), \quad (13)$$

where $w^{\min}(k) = [w_r^{\min}(k)^T \ w_d^{\min}(k)^T]^T$ and $w^{\max}(k) = [w_r^{\max}(k)^T \ w_d^{\max}(k)^T]^T$.

B. Operation cost

The operation cost under consideration is economically motivated. We assume there is no cost on operating renewable units. The operation cost of conventional units includes fuel cost, fixed-generation cost and switching cost, i. e.,

$$\begin{aligned} \ell_t(p_t(k), \delta_t(k), \delta_t(k-1)) &= C_t^T p_t(k) + C_{\text{on}}^T \delta_t(k) + \\ &C_{\text{sw}}^T |\delta_t(k) - \delta_t(k-1)|, \end{aligned} \quad (14)$$

where $C_t, C_{\text{on}}, C_{\text{sw}} \in \mathbb{R}_{\geq 0}^T$.

Typically, the purpose of storage units is to store the excess energy for future usage. This can be encouraged by including a cost on the storage power, i. e.,

$$\ell_s(p_s(k)) = C_s^T p_s(k), \quad (15)$$

where $C_s \in \mathbb{R}_{\geq 0}^S$. Hence, ℓ_s is negative if power is stored, i. e., if $p_s(k)$ is negative. In particular, this cost discourages wasting available renewable power just because it cannot be consumed by load demand instantaneously.

The total operation cost of an MG is the sum of (14) and (15), i. e.,

$$\begin{aligned} \ell(p(k), \delta_t(k), \delta_t(k-1)) &= \ell_t(p_t(k), \delta_t(k), \delta_t(k-1)) + \\ &\ell_s(p_s(k)). \end{aligned} \quad (16)$$

C. Minimax MPC

In certainty equivalence MPC, the power set-points are determined by minimizing the operation cost over the prediction horizon for a given disturbance realization. Therefore, this formulation does not rigorously account for uncertainties. In a minimax strategy, uncertainties are handled by considering their worst-case impact [9]. More precisely, a control (here, power set-points and switch statuses) is determined such that the operation cost is minimized over robustly feasible controls and at the same time maximized over possible disturbance realizations. Robustly feasible controls guarantee constraints to be satisfied for all possible disturbance realizations.

Let us consider the prediction horizon of the MM MPC as $N_p \in \mathbb{N}$. At sampling instance k , the power predicted at future step $j \in N_p$ is given by $p(k+j)$. Let us define matrices to represent profiles of variables over the prediction horizon as

$$\begin{aligned} \delta_t &:= [\delta_t(k+1) \ \cdots \ \delta_t(k+N_p)], \\ \mathbf{u} &:= [u(k+1) \ \cdots \ u(k+N_p)], \\ \mathbf{p} &:= [p(k+1) \ \cdots \ p(k+N_p)], \\ \mathbf{x} &:= [x(k+1) \ \cdots \ x(k+N_p)], \\ \mathbf{w} &:= [w(k+1) \ \cdots \ w(k+N_p)], \\ \mathbf{w}^{\min} &:= [w^{\min}(k+1) \ \cdots \ w^{\min}(k+N_p)], \\ \mathbf{w}^{\max} &:= [w^{\max}(k+1) \ \cdots \ w^{\max}(k+N_p)]. \end{aligned} \quad (17)$$

Finally, let us define the operation cost over the prediction horizon as

$$J(\mathbf{p}, \delta_t, \delta_t(k)) := \sum_{j=1}^{N_p} \ell(p(k+j), \delta_t(k+j), \delta_t(k+j-1)). \quad (18)$$

Using the notation introduced above, we first formulate the minimax MPC which includes renewable droop but no saturation in storage and conventional units.

Problem 1 (MM MPC with RES droop):

$$\min_{\mathbf{u}, \delta_t} \max_{\mathbf{w}} J(\mathbf{p}, \delta_t, \delta_t(k)), \quad (19a)$$

where $J(\cdot)$ is defined by (18), subject to the model equations

$$\begin{aligned} 0 &= \mathbf{1}^\top p(k+j) + \mathbf{1}^\top w_d(k+j), \\ p_r(k+j) &= \min(u_r(k+j) + \chi_r \rho(k+j), w_r(k+j)), \\ p_t(k+j) &= \delta_t(k+j) \wedge (u_t(k+j) + \chi_t \rho(k+j)), \\ p_s(k+j) &= u_s(k+j) + \chi_s \rho(k+j), \\ x(k+j) &= x(k+j-1) - T_s p_s(k+j), \\ j &\in \mathbb{N}_{[1, N_p]}, \end{aligned} \quad (19b)$$

initial conditions

$$x_s(k) = x_{s,0}, \quad \delta_t(k) = \delta_{t,0}, \quad (19c)$$

control constraints

$$\begin{aligned} \delta_t &\in \{0, 1\}^{T \times N_p}, \\ u^{\min} &\leq \mathbf{u} \leq u^{\max}, \end{aligned} \quad (19d)$$

uncertainty model

$$\mathbf{w}^{\min} \leq \mathbf{w} \leq \mathbf{w}^{\max}, \quad (19e)$$

power and energy constraints

$$\begin{aligned} \begin{bmatrix} \delta_t \wedge p_t^{\min} \\ p_s^{\min} \\ p_r^{\min} \end{bmatrix} &\leq \mathbf{p} \leq p^{\max}, \\ x^{\min} &\leq \mathbf{x} \leq x^{\max}, \end{aligned} \quad (19f)$$

and the condition that the control δ_t, \mathbf{u} must be feasible w. r. t. (19b), (19c), (19f) $\forall \mathbf{w} \in [\mathbf{w}^{\min}, \mathbf{w}^{\max}]$.

We now formulate the minimax MPC with droop and saturation at all the units.

Problem 2 (MM MPC with RES droop and saturation):

$$\min_{\mathbf{u}, \delta_t} \max_{\mathbf{w}} J(\mathbf{p}, \delta_t, \delta_t(k)), \quad (20a)$$

where $J(\cdot)$ is defined by (18), subject to the model equations

$$\begin{aligned} 0 &= \mathbf{1}^\top p(k+j) + \mathbf{1}^\top w_d(k+j), \\ p_r(k+j) &= \text{sat}(p_r^{\min}, u_r(k+j) + \\ &\quad \chi_r \rho(k+j), w_r(k+j)), \\ p_t(k+j) &= \delta_t(k+j) \wedge \text{sat}(p_t^{\min}, u_t(k+j) + \\ &\quad \chi_t \rho(k+j), p_t^{\max}), \\ \bar{p}_s^{\min}(k+j) &= \max(p_s^{\min}, (x(k+j-1) - x^{\max}) T_s^{-1}), \\ \bar{p}_s^{\max}(k+j) &= \min(p_s^{\max}, (x(k+j-1) - x^{\min}) T_s^{-1}), \\ p_s(k+j) &= \text{sat}(\bar{p}_s^{\min}(k+j), u_s(k+j) + \\ &\quad \chi_s \rho(k+j), \bar{p}_s^{\max}(k+j)), \\ x(k+j) &= x(k+j-1) - T_s p_s(k+j), \\ j &\in \mathbb{N}_{[1, N_p]}, \end{aligned} \quad (20b)$$

initial conditions (19c), control constraints (19d) and uncertainty model (19e), and the condition that the control δ_t, \mathbf{u} must be feasible w. r. t. (20b), (19c) $\forall \mathbf{w} \in [\mathbf{w}^{\min}, \mathbf{w}^{\max}]$.

Remark 4: In Problem 2 the constraints on the unit power and the storage unit energy are included in the saturation function and there is no need to write them explicitly.

In general, minimax problems are hard to solve. A tractable reformulation for robust integer problems without considering binary decisions in feedback is provided in [22]. But the saturation in the above problem leads to binary variables in the feedback. In previous work [7], a tractable reformulation has been found with binaries affecting the feedback. In that work, both robust feasibility and the inner maximization problem only require checking two disturbance cases – one where it is minimum at all times and one where it is maximum at all times. However, the analysis presented in [7] is not directly applicable to the above problems as it does not include RES droop and droop saturation. Therefore, it is necessary to derive tractable reformulations for the above problems.

IV. TRACTABLE REFORMULATION FOR THE MINIMAX MPC WITH SATURATION

In this section, to keep the presentation simple, we show the detailed derivation of the tractable reformulation for only Problem 2. We show that the maximum operation cost occurs for minimum disturbance $\mathbf{w} = \mathbf{w}^{\min}$. Furthermore, we show that ensuring that constraints are satisfied for $\mathbf{w} = \mathbf{w}^{\min}$ and $\mathbf{w} = \mathbf{w}^{\max}$ is sufficient to ensure that they are satisfied for all possible disturbance realizations. We also show that the MM MPC problem with saturation has a larger feasible control region than the MM MPC problem without saturation.

A. Tractable formulation

In Problem 2, the switch status of the conventional generators δ_t makes the outer minimization a mixed-integer problem. However, the disturbance \mathbf{w} cannot directly modify the switch status, which makes the inner maximization problem integer-free. Furthermore, note that all droop gains χ_s, χ_t, χ_r are non-negative. Hence the power values of all units which are not yet in saturation either increase or decrease simultaneously to achieve the power balance, or stay constant if the respective droop gain is zero. The following theorems pinpoint the disturbance sequences that have to be considered (instead of all possible sequences) with regard to robust feasibility and the maximum cost.

Theorem 1: In Problem 2, given non-negative droop gains χ_s, χ_t, χ_r , the set of feasible controls (δ_t, \mathbf{u}) reduces to the set of controls which are feasible for disturbance realizations $\mathbf{w} = \mathbf{w}^{\min}$ and $\mathbf{w} = \mathbf{w}^{\max}$.

Proof: See Appendix -A and -B.

Theorem 2: In Problem 2, given non-negative droop gains χ_s, χ_t, χ_r , the worst-case operation cost corresponds to the disturbance realization $\mathbf{w} = \mathbf{w}^{\min}$.

Proof: See Appendix -A and -C.

Using Theorem 1 and 2, the MM MPC Problem 2 can be equivalently stated as

Problem 3 (Tractable MM MPC):

$$\min_{\mathbf{u}, \delta_t} J(\mathbf{p}, \delta_t, \delta_t(k))|_{\mathbf{w}=\mathbf{w}^{\min}}, \quad (21)$$

where $J(\cdot)$ is defined by (18), subject to the model equations (20b), initial conditions (19c), control constraints (19d), and the condition that the control δ_t, \mathbf{u} must be feasible w.r.t. (19c), (20b) for $\mathbf{w} = \mathbf{w}^{\min}$ and for $\mathbf{w} = \mathbf{w}^{\max}$.

Remark 5: The $\text{sat}(\cdot, \cdot, \cdot)$ in the current formulation can be included with additional binary variables as in [27], which may increase computational complexity.

B. Enhancing feasibility

The robust feasibility requirement of the MM MPC optimization problem restricts the set of admissible controls, which leads to conservative power set-points. In Problem 2, constraints on the power and energy are included as saturation instead of hard limits $\mathbf{p} \in [p^{\min}, p^{\max}]$, $\mathbf{x} \in [x^{\min}, x^{\max}]$ as in Problem 1. It is shown here that this enlarges the feasible control space.

Theorem 3: Any feasible solution to Problem 1 is a feasible solution to Problem 2. However, the converse does not hold in general. Furthermore, a feasible solution for Problems 1 and 2 is associated with the same cost value in both problems.

Proof: An alternative way to express Problem 1 is by augmenting Problem 2 with the following constraints:

$$\begin{aligned} u_r(k+j) + \chi_r \rho(k+j) &\geq p_r^{\min}, \\ u_s(k+j) + \chi_s \rho(k+j) &\in [p_s^{\min}, p_s^{\max}], \\ x(k+j-1) - T_s(u_s(k+j) + \chi_s \rho(k+j)) &\in [x^{\min}, x^{\max}], \\ \delta_t(k+j) \wedge (u_s(k+j) + \chi_s \rho(k+j)) &\in [p_t^{\min}, p_t^{\max}]. \end{aligned}$$

Essentially, these are constraints preventing units from going into saturation. Therefore, a feasible solution to the more stringent Problem 1 is a feasible solution to Problem 2. As the problems differ only in constraints, not in the cost function, the feasible solution is associated with the same cost value in both problems.

But the vice-versa does not hold in general. As a counter-example, consider a scenario when the power set-points of units 1 and 2 are $u_1(k+j) = p_1^{\min}$ and $u_2(k+j) = p_2^{\max}$. Hence, without saturation, $p_1(k+j) = p_1^{\min} + \chi_1 \rho(k+j)$ and $p_2(k+j) = p_2^{\max} + \chi_2 \rho(k+j)$. The power constraints $[p^{\min}, p^{\max}]$ in Problem 1 can be satisfied if and only if $\rho(k+j) = 0$, i.e., a power imbalance caused by an unknown disturbance in the system cannot be compensated. On the other hand, when units are allowed to saturate, $\rho(k+j)$ can become positive and unit 1 can increase its power output, $p_1(k+j) > p_1^{\min}$, to compensate a negative power imbalance, while the power output of unit 2 stays constant at $p_2(k+j) = p_2^{\max}$. Similarly, a positive imbalance can be compensated by unit 1 keeping its power at $p_1(k+j) = p_1^{\min}$ and unit 2 decreasing its power, $p_2(k+j) < p_2^{\max}$.

V. CASE STUDY

In this section, we demonstrate the benefits of the proposed saturation-based robust controller assuming the MG with high share of renewable infeed shown in Figure 2. The MG consists of a wind turbine, a PV power plant, a storage unit, a conventional unit and a load. Power and energy limits of the units are posed in Table I together with the droop gains and

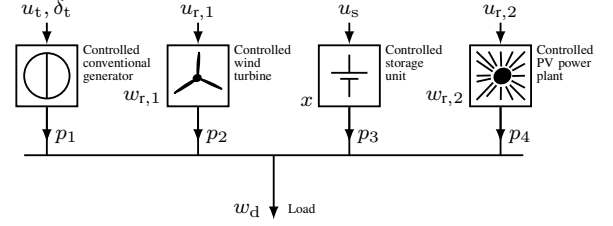


Figure 2. Test microgrid topology

Table I
UNIT PARAMETERS AND WEIGHTS OF COST FUNCTION.

Parameter	Value	Weight	Value
$[u_t^{\min} u_s^{\min} u_{r,1}^{\min} u_{r,2}^{\min}]$	$[-5 -5 -5 -5]$ pu	C_t	1
$[u_t^{\max} u_s^{\max} u_{r,1}^{\max} u_{r,2}^{\max}]$	$[5 5 5 5]$ pu	C_{on}	0.2
$[p_t^{\min} p_s^{\min} p_{r,1}^{\min} p_{r,2}^{\min}]$	$[0.2 -1 0 0]$ pu	C_{sw}	0.3
$[p_t^{\max} p_s^{\max}]$	$[1 1]$ pu	C_s	0.9
$[x_{\min} x_{\max}]$	$[0 6]$ pu h		
x^0	2 pu h		
$[\chi_t \chi_s \chi_{r,1} \chi_{r,2}]$	$[1 1 1 1]$		

the weights of the cost function. Note that c_s is smaller than c_t to discourage charging the storage with conventional power.

The EMS sampling time is chosen to be 15 min and the prediction horizon of the MPC is 8 h, i.e., $N_p = 32$. The simulation horizon is 6 days, i.e., $N_s = 576$. The model and the controllers are implemented in Matlab[®]2015a. The MPC optimization is formulated using YALMIP [28] and solved with Gurobi 8.1.1 [29].

The available renewable infeed is generated based on real measurement data provided by the Atmospheric Radiation Measurement (ARM) Climate Research Facility [30], located at Graciosa Airport, Azores, Portugal. The robust intervals for the disturbance are typically generated using a forecaster [31], [26]. As this generation is out of the scope of the paper, we assume hypothetical robust intervals given by minimum and maximum disturbance, $w^{\min}(k)$ and $w^{\max}(k)$. The resulting robust intervals are highlighted in Figure 3. The robust interval for the load demand was generated in a similar fashion and is also illustrated in Figure 3.

For the simulations, we consider the *worst-case* disturbance realization, $\mathbf{w} = \mathbf{w}^{\min}$, as this corresponds to the worst-case open-loop operation cost (see Theorem 2).

A. Prescient controller

A prescient MPC is a hypothetical controller which has perfect future knowledge of the available renewable infeed and the load demand. In particular, for the worst-case disturbance realization \mathbf{w}^{\min} , the corresponding worst-case prescient MPC is formulated based on Problem 2 as follows. The uncertainty model (19e) is replaced by $\mathbf{w} = \mathbf{w}^{\min}$ and, accordingly, the robust feasibility condition is replaced by the condition of feasibility for $\mathbf{w} = \mathbf{w}^{\min}$. The closed-loop simulation with worst-case disturbance realization and worst-case prescient MPC is visualized in Figure 3. The corresponding open-loop cost values predicted each time the worst-case prescient MPC problem is solved are included in Figure 4.

Remark 6: The open-loop cost value corresponding to the worst-case prescient controller is a lower bound for the cost value corresponding to the MM MPC Problem 2. This can be easily deduced from Theorems 1 and 2. In fact, the open-loop cost of the prescient MPC is a lower bound for the open-loop cost value corresponding to any conceivable robust MPC controller. This can be inferred by noting that the prescient MPC is able to select an optimal physically possible power output profile $p(k+j)$, $j \in \mathbb{N}_{[1, N_p]}$, and a corresponding switch status profile.

B. Open-loop comparison

Here, we compare open-loop performance of different MPC controllers for given initial energy levels and switch statuses and identical robust forecast intervals. A collection of 576 variations of this data is obtained from the closed-loop simulation with the worst-case prescient MPC.

Here, we define the labels for the different considered MPC controllers:

- 1) Prescient: worst-case prescient MPC,
- 2) MM: Problem 1 with $\chi_r = 0$,
- 3) Sat. MM: Problem 2 with $\chi_r = 0$,
- 4) RES-droop MM: Problem 1 with $\chi_r > 0$,
- 5) Sat. RES-droop MM: Problem 2 with $\chi_r > 0$.

Figure 4 shows the open-loop cost predicted by these controllers. We can observe:

- Sat. MM MPC does not reduce the predicted cost value compared to MM MPC.
- RES-droop MM MPC reduces the cost value compared to MM MPC during periods of high share of renewable infeed, e.g., between days 4 and 6.
- Sat. RES-droop MM MPC provides an equal or lower cost than the remaining controllers. This illustrates that Sat. RES-droop MM MPC increases the feasible region compared to RES-droop MM MPC and thereby achieves a lower open-loop cost (Theorem 3).

These items suggest a synergy between the features RES droop and saturation of *all* units. In fact, the cost value of Sat. RES-droop MM MPC and the worst-case prescient MPC apparently coincide over the entire simulation horizon. This indicates that no conceivable robust MPC and low-level control combination could perform better in this case study as far as open-loop prediction is concerned (see Remark 6).

The average (per sample over the 6-day period) predicted cost and average predicted RES and conventional infeed of the controllers are shown in Table II. Here, differences in average predicted RES infeed energies can be observed, while average predicted conventional infeed is identical for all MPC controllers. This indicates that lower predicted cost values are predominantly attributed to harvesting more energy from RES thus boosting storage energy level at the end of the prediction horizon.

C. Closed-loop simulation

Closed-loop simulations with different MPC controllers are performed over a 6-day period, comprising $N_s = 576$ sampling instances. These closed-loop simulations are performed

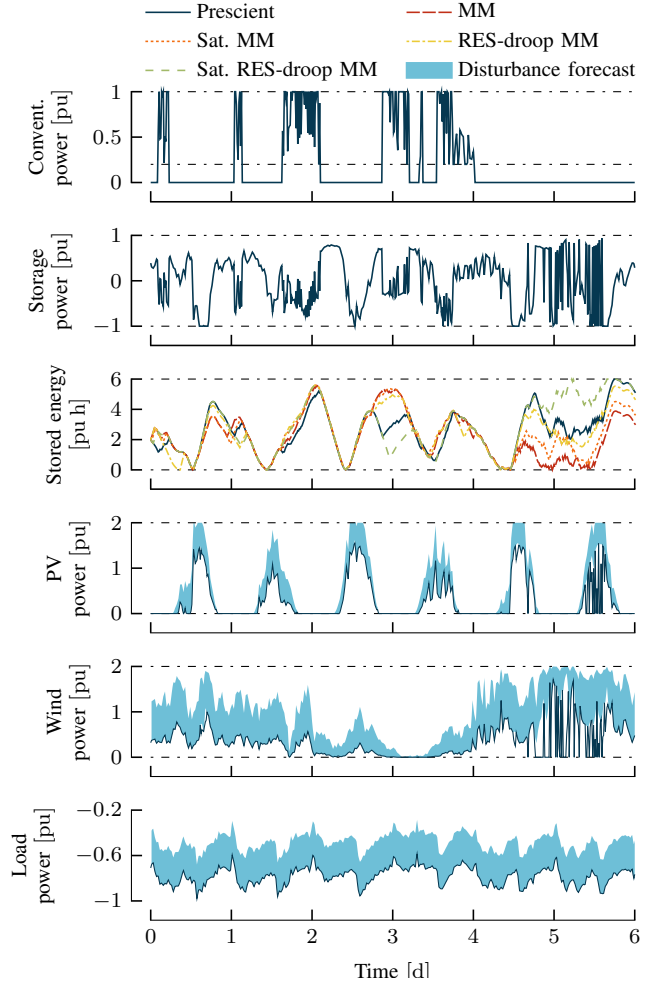


Figure 3. Closed-loop simulation with the worst case disturbance realization. For clarity, the plots corresponding to controllers other than prescient MPC are only shown in the case of stored energy.

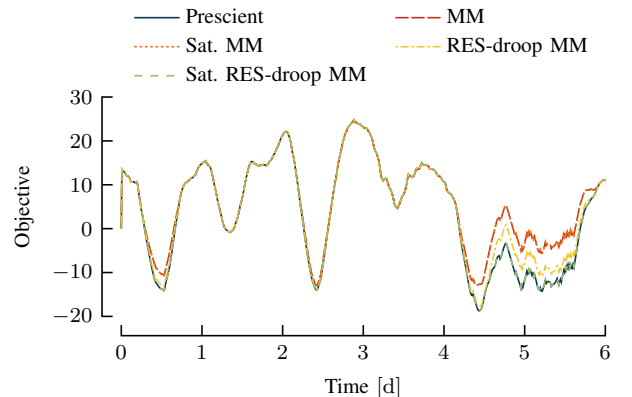


Figure 4. Predicted MPC cost for 576 different initial conditions and robust forecast intervals. The sequence of variations of this data stems from a closed-loop simulation with the worst-case prescient controller.

Table II
COMPARISON OF AVERAGE OPEN-LOOP MPC PERFORMANCE FOR 576
INITIAL CONDITIONS (PER-SAMPLE).

	Cost	RES [pu h]	Convent. [pu h]
Prescient	0.121	0.169	0.0136
MM	0.188	0.150	0.0136
Sat. MM	0.188	0.150	0.0136
RES-droop MM	0.144	0.162	0.0136
Sat. RES-droop MM	0.121	0.169	0.0136

Table III
COMPARISON OF CLOSED-LOOP PERFORMANCE FOR WORST-CASE
DISTURBANCE REALIZATION (PER-SAMPLE EXCEPT SWITCHINGS).

	Cost	RES [pu h]	Convent. [pu h]	Switch. [#]
Prescient	0.225	0.155	0.0466	12
MM	0.255	0.149	0.0490	22
Sat. MM	0.253	0.150	0.0488	14
RES-droop MM	0.233	0.154	0.0472	18
Sat. RES-droop MM	0.224	0.155	0.0466	10

assuming the *worst-case* disturbance realization $w(k) = w^{\min}(k)$. Figure 3 includes energy profiles resulting for different MPC controllers. Here, we can observe that the Sat. RES-droop MM MPC tends to harvest more energy resulting in higher energy levels.

Based on the total operation cost (16) and the cost definition in Problem 2, closed-loop per-sample cost values are calculated over the entire $N_s = 576$ samples in the simulation by

$$J^{\text{closed-loop}} := 1/N_s \sum_{k=1}^{N_s} \ell(p(k), \delta_t(k), \delta_t(k-1)), \quad (22)$$

where $\delta_t(0)$ are the given initial switch statuses and $p(k)$, $\delta_t(k)$, $k \in \{1, \dots, N_s\}$, are the variable evolutions resulting from the respective simulation. Per-sample RES and conventional infeed energies are defined in the same manner. The resulting values for different controller are shown in Table III. The Sat. RES-droop MM MPC and the prescient MPC result in the same Per-sample RES and conventional infeed energies. The variation in the per-sample cost results from the higher number of switching in prescient MPC compared to Sat. RES-droop MM MPC. The considered MPC formulation uses a finite horizon and hence, it is not guaranteed to deliver the optimal closed-loop performance. Furthermore, here the MPC formulation can have multiple optimal solutions with same optimal cost which could explain different control decisions. Also note that – contrary to open-loop prediction – not all closed-loop conventional infeed energies are identical.

VI. CONCLUSIONS

In this paper, we have demonstrated that the conservativeness in minimax MPC of a microgrid can be reduced by including saturations in droop control and droop control of renewable energy systems. We have derived a tractable reformulation of the optimal control problem over a finite prediction horizon. This reformulation is based on analytical solutions for the disturbance maximizing the cost function,

independently of the control. In a case study, we have observed that, compared to classical minimax MPC, including droop control of RES provides a benefit, and including both droop control of RES and saturations in droop control of all units can reduce conservativeness of the minimax MPC.

We think evident future work is to extend our model by a detailed battery model and an electrical network. Also, we would like to further investigate the effects related to power sharing of RES and extend the research to include piecewise-affine droop curves or time varying droop parameters. Furthermore, we plan to extend the robust MPC in the following ways. First, we suppose that our analysis can be extended to more general convex or monotonic costs. Second, we think the conservativeness of the robust MPC can be reduced, for example by formulating a multi-objective problem. Finally, the impact of saturation on computational complexity should be studied.

A. Preliminaries and lemmas used for proving Theorems 1 and 2

In the following, we prepare the ground for proving Theorems 1 and 2, which deal with feasibility and the worst-case cost, respectively. For evaluating feasibility, we will introduce a measure which allows us to decide whether a control is feasible or not. We want this measure to be always well-defined – also when the control is not feasible. For this purpose, we reformulate Problem 2 and use a relaxation.

For the proofs, it is convenient to solve the algebraic equations corresponding to the power balance and droop control with saturation for $\rho(k+j)$. Therefore, we define a $\rho(k+j)$ -candidate explicitly as a function of $u(k+j)$, $\delta_t(k+j)$, $x(k+j-1)$, $w(k+j)$, $j \in \mathbb{N}_{[1, N_p]}$. The following definitions and Lemma 1 are concerned with this $\rho(k+j)$ -candidate function and its properties when we assume that $u(k+j)$, $\delta_t(k+j)$, $x(k+j-1)$, $w(k+j)$ are independent variables. Based on the function and its established properties, Lemma 2 and the proofs thereafter analyze the evolution of variables over the prediction horizon $j \in \mathbb{N}_{[1, N_p]}$. Please note that we sometimes ease notation by omitting the time indexes $k+j$ and $k+j-1$.

We denote the droop control laws with saturation (8), (9), (10) by functions of the independent variables by writing $p_r(u_r, w_r, \rho)$, $p_t(u_t, \delta_t, \rho)$, $p_s(u_s, x, \rho)$, respectively. Note that one of the important facts about these functions is: for any fixed values of the other variables, they are monotonically increasing in ρ . Let us define auxiliary lower and upper bounds on ρ , so that for values of ρ exceeding those bounds it is guaranteed that all units (except those with zero droop gain, the power output of which is not affected by ρ) are in lower respectively in upper saturation. These bounds are determined by the range of possible power to power-setpoint differences, i. e.,

$$\rho^{\min} := \min_{i \in \mathbb{N}_{[1, T+S+R]} \setminus \{i | \chi_i = 0\}} \frac{p_i^{\min} - u_i^{\max}}{\chi_i}, \quad (23a)$$

$$\rho^{\max} := \max_{i \in \mathbb{N}_{[1, T+S+R]} \setminus \{i | \chi_i = 0\}} \frac{p_i^{\max} - u_i^{\min}}{\chi_i}. \quad (23b)$$

Because power output of units is constant for ρ outside of these bounds, we can w.l.o.g. add the auxiliary constraint

$$\rho^{\min} \leq \rho(k+j) \leq \rho^{\max} \quad \forall j \in \mathbb{N}_{[1, N_p]} \quad (24)$$

to (20b) in Problem 2. This, in turn, enables us to augment (1) by an additional term. That is, we define

$$\begin{aligned} \tilde{p}_{\text{tot}}(u, \delta_t, x, w, \rho) := & \\ & \min(0, \rho - \rho^{\min}) + \max(0, \rho - \rho^{\max}) + \\ & \mathbf{1}^\top p_t(u_t, \delta_t, \rho) + \mathbf{1}^\top p_s(u_s, x, \rho) + \mathbf{1}^\top p_r(u_r, w_r, \rho) + \mathbf{1}^\top w_d \end{aligned} \quad (25)$$

to ensure that, for any combination of u , δ_t , x , w , we can always find a $\rho \in \mathbb{R}$ which satisfies

$$\tilde{p}_{\text{tot}}(u, \delta_t, x, w, \rho) = 0. \quad (26)$$

Accordingly, (26) is identical to (1) only as long as (24) holds, but the function $\tilde{p}_{\text{tot}}(\cdot, \rho)$ by itself is defined for $\rho \in \mathbb{R}$ and – because of the additional term – is a surjective function of ρ . It is also piecewise affine, continuous and monotonically increasing. It may be constant on some intervals. However, it is easy to see that any interval where $\tilde{p}_{\text{tot}}(\cdot, \rho)$ is constant fulfills the following. 1) It is contained in $[\rho^{\min}, \rho^{\max}]$. 2) All unit power functions are constant on it. If $\tilde{p}_{\text{tot}}(\cdot) = 0$ is located on a constant interval, the lower control layers would settle at a certain ρ . W.l.o.g., let us assume that always the maximum possible ρ is selected and define a function that provides a ρ -solution of (26) as

$$\tilde{\rho}(u, \delta_t, x, w) := \max_{\rho \in \mathbb{R}} \rho \quad \text{s.t.} \quad \tilde{p}_{\text{tot}}(u, \delta_t, x, w, \rho) = 0. \quad (27)$$

Using this function to define a $\rho(k+j)$ -candidate, the constraint (24), and the aforementioned functions to express the droop control laws with saturation, the robust optimal control Problem 2 can be equivalently stated as

Problem 4:

$$\min_{\mathbf{u}, \delta_t} \max_{\mathbf{w}} J(\mathbf{p}, \delta_t, \delta_t(k)), \quad (28a)$$

where $J(\cdot)$ is defined by (18), subject to the model equations consisting of (25), (27) and

$$\begin{aligned} p_r(k+j) &= p_r(u_r(k+j), w_r(k+j), \rho(k+j)), \\ p_t(k+j) &= p_t(u_t(k+j), \delta_t(k+j), \rho(k+j)), \\ p_s(k+j) &= p_s(u_s(k+j), x(k+j-1), \rho(k+j)), \\ x(k+j) &= x(k+j-1) - \mathbb{T}_s p_s(k+j), \\ \rho(k+j) &= \tilde{\rho}(u(k+j), \delta_t(k+j), x(k+j-1), w(k+j)), \\ \rho^{\min} &\leq \rho(k+j) \leq \rho^{\max}, \\ j &\in \mathbb{N}_{[1, N_p]}, \end{aligned} \quad (28b)$$

the initial conditions (19c), control constraints (19d) and uncertainty model (19e), and the condition that the control δ_t , \mathbf{u} must be feasible w.r.t. (25), (27), (28b), (19c) $\forall \mathbf{w} \in [\mathbf{w}^{\min}, \mathbf{w}^{\max}]$.

Lemma 1: $\tilde{\rho}(u, \delta_t, x, w)$ is monotonically decreasing in x and w . That is, consider values of the respective variables corresponding to two scenarios, $x^{(1)}$, $x^{(2)}$ and $w^{(1)}$ and $w^{(2)}$.

The remaining variables are supposed to have the same values in both scenarios. Then,

$$x^{(2)} \geq x^{(1)} \implies \tilde{\rho}(u, \delta_t, x^{(2)}, w) \leq \tilde{\rho}(u, \delta_t, x^{(1)}, w), \quad (29a)$$

$$w^{(2)} \geq w^{(1)} \implies \tilde{\rho}(u, \delta_t, x, w^{(2)}) \leq \tilde{\rho}(u, \delta_t, x, w^{(1)}). \quad (29b)$$

Proof: Proving (29a) makes use of the fact

$$\begin{aligned} x^{(2)} \geq x^{(1)} \implies \\ \tilde{p}_{\text{tot}}(u, \delta_t, x^{(2)}, w, \rho) \geq \tilde{p}_{\text{tot}}(u, \delta_t, x^{(1)}, w, \rho) \quad \forall \rho \in \mathbb{R}, \end{aligned} \quad (30)$$

which can be deduced as follows: \bar{p}_s^{\min} and \bar{p}_s^{\max} given by (10a) are monotonically increasing in x ; therefore, noting that $\text{sat}(p^{\min}, p, p^{\max})$ is monotonically increasing in p^{\min} and p^{\max} , p_s given by (10b) is monotonically increasing in x ; therefore, \tilde{p}_{tot} given by (25) is monotonically increasing in x .

According to (27),

$$\begin{aligned} \tilde{\rho}^{(1)} := \tilde{\rho}(u, \delta_t, x^{(1)}, w) = \max \rho \\ \text{s.t.} \quad \tilde{p}_{\text{tot}}(u, \delta_t, x^{(1)}, w, \rho) = 0, \end{aligned} \quad (31a)$$

$$\begin{aligned} \tilde{\rho}^{(2)} := \tilde{\rho}(u, \delta_t, x^{(2)}, w) = \max \rho \\ \text{s.t.} \quad \tilde{p}_{\text{tot}}(u, \delta_t, x^{(2)}, w, \rho) = 0, \end{aligned} \quad (31b)$$

which satisfy

$$\tilde{p}_{\text{tot}}(u, \delta_t, x^{(1)}, w, \tilde{\rho}^{(1)}) = 0, \quad (32a)$$

$$\tilde{p}_{\text{tot}}(u, \delta_t, x^{(2)}, w, \tilde{\rho}^{(2)}) = 0. \quad (32b)$$

As a consequence of (30) and (32b) we know that

$$\tilde{p}_{\text{tot}}(u, \delta_t, x^{(1)}, w, \tilde{\rho}^{(2)}) \leq \tilde{p}_{\text{tot}}(u, \delta_t, x^{(2)}, w, \tilde{\rho}^{(2)}) = 0. \quad (33)$$

By definition (31a), $\tilde{\rho}^{(1)}$ is the maximum ρ for which $\tilde{p}_{\text{tot}}(u, \delta_t, x^{(1)}, w, \rho) = 0$. Therefore, if we suppose $\tilde{\rho}^{(2)} > \tilde{\rho}^{(1)}$, this would imply

$$\tilde{p}_{\text{tot}}(u, \delta_t, x^{(1)}, w, \tilde{\rho}^{(2)}) \neq 0,$$

and (32a) and the fact that $\tilde{p}_{\text{tot}}(u, \delta_t, x^{(1)}, w, \rho)$ is a monotonically increasing function of ρ would imply

$$\tilde{p}_{\text{tot}}(u, \delta_t, x^{(1)}, w, \tilde{\rho}^{(2)}) \geq \tilde{p}_{\text{tot}}(u, \delta_t, x^{(1)}, w, \tilde{\rho}^{(1)}) = 0.$$

Consequently, $\tilde{p}_{\text{tot}}(u, \delta_t, x^{(1)}, w, \tilde{\rho}^{(2)}) > 0$ would be implied, which contradicts (33). This concludes the proof of (29a).

Proving (29b) makes use of the fact

$$\begin{aligned} w^{(2)} \geq w^{(1)} \implies \\ \tilde{p}_{\text{tot}}(u, \delta_t, x, w^{(2)}, \rho) \geq \tilde{p}_{\text{tot}}(u, \delta_t, x, w^{(1)}, \rho) \quad \forall \rho \in \mathbb{R}, \end{aligned} \quad (34)$$

which can be deduced as follows: noting that $\text{sat}(p^{\min}, p, p^{\max})$ is monotonically increasing in p^{\min} and p^{\max} , p_r given by (8) is monotonically increasing in w_r ; therefore, \tilde{p}_{tot} given by (25) is monotonically increasing in w_r ; since \tilde{p}_{tot} is also monotonically increasing in w_d , it is monotonically increasing in w .

Lemma 2: Consider Problem 4 and two scenarios with common control actions $u(k+j)$, $\delta_t(k+j)$ but different

disturbance forecasts $w^{(1)}(k+j)$ and $w^{(2)}(k+j)$. For a given j , if

$$w^{(2)}(k+j) \geq w^{(1)}(k+j), \quad (35a)$$

$$x^{(2)}(k+j-1) \geq x^{(1)}(k+j-1), \quad (35b)$$

then

$$\rho^{(2)}(k+j) \leq \rho^{(1)}(k+j), \quad (36a)$$

$$p_t^{(2)}(k+j) \leq p_t^{(1)}(k+j), \quad (36b)$$

$$x^{(2)}(k+j) \geq x^{(1)}(k+j). \quad (36c)$$

Proof: Defining an auxiliary storage power demand $\tilde{p}_s(k+j)$ that does not consider state of charge-dependent power limits, the storage model (10), (3b) can be transformed into a model composed of

$$\tilde{p}_s(k+j) := \text{sat}(p_s^{\min}, u_s(k+j) + \chi_s \rho(k+j), p_s^{\max}), \quad (37a)$$

$$x(k+j) = \text{sat}(x^{\min}, x(k+j-1) - T_s \tilde{p}_s(k+j), x^{\max}) \quad (37b)$$

and

$$p_s(k+j) = 1/T_s (x(k+j-1) - x(k+j)). \quad (37c)$$

From (35a), (35b) and Lemma 1 follows (36a). From (36a) and (9) and with $\chi \geq 0$ follows (36b), and from (36a) and (37a) follows

$$\tilde{p}_s^{(2)}(k+j) \leq \tilde{p}_s^{(1)}(k+j). \quad (38)$$

Using this in (37b) directly leads to (36c).

Having derived Lemmas 1 and 2, we can now use them to prove Theorems 1 and 2.

B. Proof of Theorem 1

Proof: Here, we again refer to the vector respectively matrix definitions (17) for profiles over the prediction horizon. We need to show that, for given initial conditions, a control is robustly feasible in the sense of Problem 2 for all possible disturbance realizations $\mathbf{w} \in [\mathbf{w}^{\min}, \mathbf{w}^{\max}]$ if and only if it is feasible for disturbance realizations $\mathbf{w} = \mathbf{w}^{\min}$ and $\mathbf{w} = \mathbf{w}^{\max}$.

Consider Problem 4 defined above, which is equivalent to Problem 2. Note that for a relaxed problem – where (24) is abandoned – any control, $u^{\min} \leq \mathbf{u} \leq u^{\max}$, is feasible for any disturbance and initial conditions. In particular, $\rho(k+j)$ is always well-defined, even if it is not contained in the interval $[\rho^{\min}, \rho^{\max}]$. Therefore, for the relaxed problem, consider the sequence $\boldsymbol{\rho} := [\rho(k+1) \dots \rho(k+N_p)]$ which is uniquely determined by a given initial state $x'(k)$ and initial switch statuses $\delta'_t(k)$, control $\boldsymbol{\delta}'_t := [\delta'_t(k+1) \dots \delta'_t(k+N_p)]$, $\mathbf{u}' := [u'(k+1) \dots u'(k+N_p)]$ and disturbance forecast \mathbf{w} . Whether $\boldsymbol{\rho}$ satisfies $\rho^{\min} \leq \rho(k+j) \leq \rho^{\max} \forall j \in \mathbb{N}_{[1, N_p]}$ indicates if also in the context of Problem 4 the given control is feasible for the given disturbance forecast and initial conditions.

Therefore, we need to show that for any given $x'(k) \in [x^{\min}, x^{\max}]$, $\delta'_t(k) \in \{0, 1\}^T$, $\boldsymbol{\delta}'_t \in \{0, 1\}^{T \times N_p}$, $\mathbf{u}' \in [u^{\min}, u^{\max}]$, it holds that

$$\rho^{\min} \leq \boldsymbol{\rho} \begin{cases} x(k)=x'(k), \\ \delta_t=\delta'_t, \\ \mathbf{u}=\mathbf{u}', \\ \mathbf{w} \end{cases} \leq \rho^{\max} \quad \forall \mathbf{w} \in [\mathbf{w}^{\min}, \mathbf{w}^{\max}],$$

if and only if

$$\rho^{\min} \leq \boldsymbol{\rho} \begin{cases} x(k)=x'(k), \\ \delta_t=\delta'_t, \\ \mathbf{u}=\mathbf{u}', \\ \mathbf{w} \end{cases} \leq \rho^{\max} \quad \begin{array}{l} \text{for } \mathbf{w} = \mathbf{w}^{\min} \\ \text{and } \mathbf{w} = \mathbf{w}^{\max}. \end{array} \quad (39)$$

Note that the initial switch statuses $\delta'_t(k)$ are missing in the condition blocks because they only impact the cost but not the constraints of the problem.

The only if-part is trivial as \mathbf{w}^{\min} and \mathbf{w}^{\max} are already included in the interval $[\mathbf{w}^{\min}, \mathbf{w}^{\max}]$. To prove the if-part, consider two scenarios with disturbance realizations $\mathbf{w}^{(1)} \leq \mathbf{w}^{(2)}$. Both scenarios assume the same control actions over the prediction horizon and identical initial conditions, i. e.,

$$x^{(1)}(k) = x^{(2)}(k), \quad \delta_t^{(1)}(k) = \delta_t^{(2)}(k), \quad (40a)$$

$$\delta_t^{(1)}(k+j) = \delta_t^{(2)}(k+j) \quad \forall j \in \mathbb{N}_{[1, N_p]}, \quad (40b)$$

$$u^{(1)}(k+j) = u^{(2)}(k+j) \quad \forall j \in \mathbb{N}_{[1, N_p]}, \quad (40c)$$

$$w^{(1)}(k+j) \leq w^{(2)}(k+j) \quad \forall j \in \mathbb{N}_{[1, N_p]}. \quad (40d)$$

From iteratively applying Lemma 2 follows

$$\rho^{(1)}(k+j) \geq \rho^{(2)}(k+j) \quad \forall j \in \mathbb{N}_{[1, N_p]}. \quad (41)$$

To summarize, if the evolution of the other variables is fixed, we have $\mathbf{w}^{(1)} \leq \mathbf{w}^{(2)} \implies \boldsymbol{\rho}^{(1)} \geq \boldsymbol{\rho}^{(2)}$. Now substitute $\mathbf{w}^{(1)} = \mathbf{w}^{\min}$ and $\mathbf{w}^{(2)} = \mathbf{w}$ and denote the respective $\boldsymbol{\rho}^{(1)} =: \boldsymbol{\rho}_{|\mathbf{w}^{\min}}$ and $\boldsymbol{\rho}^{(2)} =: \boldsymbol{\rho}_{|\mathbf{w}}$. Consequently, $\mathbf{w}^{\min} \leq \mathbf{w} \implies \boldsymbol{\rho}_{|\mathbf{w}^{\min}} \geq \boldsymbol{\rho}_{|\mathbf{w}}$. Combining this with the result of the substitution $\mathbf{w}^{(1)} = \mathbf{w}$ and $\mathbf{w}^{(2)} = \mathbf{w}^{\max}$ and defining $\boldsymbol{\rho}_{|\mathbf{w}^{\max}}$ accordingly gives

$$\mathbf{w}^{\min} \leq \mathbf{w} \leq \mathbf{w}^{\max} \implies \boldsymbol{\rho}_{|\mathbf{w}^{\max}} \leq \boldsymbol{\rho}_{|\mathbf{w}} \leq \boldsymbol{\rho}_{|\mathbf{w}^{\min}}. \quad (42)$$

The condition on the left side of this implication is obviously true, and so we can state that $\boldsymbol{\rho}_{|\mathbf{w}}$ is bounded by $\boldsymbol{\rho}_{|\mathbf{w}^{\max}}$ and $\boldsymbol{\rho}_{|\mathbf{w}^{\min}}$. If, in turn, each of these bounds is bounded by ρ^{\min} and ρ^{\max} , then $\boldsymbol{\rho}_{|\mathbf{w}}$ is bounded by ρ^{\min} and ρ^{\max} . This represents the if-part of (39) and completes the proof.

C. Proof of Theorem 2

Proof: Using the same matrix respectively vector definitions as before, we need to show that, for any given initial state $x'(k)$ and switch statuses $\delta'_t(k)$ as well as control actions $\boldsymbol{\delta}'_t$ and \mathbf{u}' , solving the inner maximization problem in (20) reduces to

$$\max_{\mathbf{w} \in [\mathbf{w}^{\min}, \mathbf{w}^{\max}]} J \begin{cases} x(k)=x'(k), \\ \delta_t(k)=\delta'_t(k), \\ \delta_t=\delta'_t, \\ \mathbf{u}=\mathbf{u}', \\ \mathbf{w} \end{cases} = J \begin{cases} x(k)=x'(k), \\ \delta_t(k)=\delta'_t(k), \\ \delta_t=\delta'_t, \\ \mathbf{u}=\mathbf{u}', \\ \mathbf{w}=\mathbf{w}^{\min} \end{cases}. \quad (43)$$

Consider two scenarios with disturbance realizations $\mathbf{w}^{(1)} \leq \mathbf{w}^{(2)}$ as in (40). From iteratively applying Lemma 2 follows

$$p_t^{(1)}(k+j) \geq p_t^{(2)}(k+j) \quad \forall j \in \mathbb{N}_{[1, N_p]}, \quad (44a)$$

$$x^{(1)}(k+j) \leq x^{(2)}(k+j) \quad \forall j \in \mathbb{N}_{[1, N_p]}. \quad (44b)$$

Note that in particular $x^{(1)}(k + N_p) \leq x^{(2)}(k + N_p)$. With the storage dynamics (3b), the cost in (20) can be equivalently expressed as

$$J = -\frac{C_s^T}{T_s}(x(k + N_p) - x(k)) + \sum_{j=1}^{N_p} (C_t^T p_t(k + j) + C_{on}^T \delta_t(k + j) + C_{sw}^T |\delta_t(k + j) - \delta_t(k + j - 1)|). \quad (45)$$

With (40b), (40a) and (44), and recalling that C_s , C_t are positive, it follows that

$$J^{(1)} \geq J^{(2)}. \quad (46)$$

To summarize, if the evolution of the other variables is fixed, we have $\mathbf{w}^{(1)} \leq \mathbf{w}^{(2)} \implies J^{(1)} \geq J^{(2)}$. Now substitute $\mathbf{w}^{(1)} = \mathbf{w}^{\min}$ and $\mathbf{w}^{(2)} = \mathbf{w}$ and denote the respective $J^{(1)} =: J_{|\mathbf{w}^{\min}}$ and $J^{(2)} =: J_{|\mathbf{w}}$. Consequently, $\mathbf{w}^{\min} \leq \mathbf{w} \implies J_{|\mathbf{w}^{\min}} \geq J_{|\mathbf{w}}$. The condition on the left side of this implication is obviously true, and so we can state that $J_{|\mathbf{w}^{\min}}$ is an upper bound for $J_{|\mathbf{w}}$. It is attained by inserting $\mathbf{w} = \mathbf{w}^{\min}$, and so \mathbf{w}^{\min} maximizes $J_{|\mathbf{w}}$.

REFERENCES

- [1] REN21 Secretariat, "Renewables 2018 global status report," Renewable Energy Policy Network for the 21st Century (REN21), c/o UN Environment, 1 rue Miollis, Building VII, 75015 Paris, France, Tech. Rep., 2018.
- [2] S. Parhizi, H. Lotfi, A. Khodaei, and S. Bahrarnirad, "State of the art in research on microgrids: A review," *IEEE Access*, vol. 3, pp. 890–925, 2015.
- [3] IEEE PES Task Force on Microgrid Stability Analysis, "Microgrid Stability Definitions, Analysis, and Modeling (technical report PES-TR66)," IEEE Power & Energy Society, Tech. Rep., Apr. 2018.
- [4] J. Schiffer, R. Ortega, A. Astolfi, J. Raisch, and T. Sezi, "Conditions for stability of droop-controlled inverter-based microgrids," *Automatica*, vol. 50, no. 10, pp. 2457–2469, 2014. [Online]. Available: <http://www.sciencedirect.com/science/article/pii/S0005109814003100>
- [5] M. F. Zia, E. Elbouchikhi, and M. Benbouzid, "Microgrids energy management systems: A critical review on methods, solutions, and prospects," *Applied Energy*, vol. 222, pp. 1033–1055, 2018. [Online]. Available: <http://www.sciencedirect.com/science/article/pii/S0306261918306676>
- [6] A. Parisio, E. Rikos, and L. Glielmo, "A model predictive control approach to microgrid operation optimization," *IEEE Trans. Control Syst. Technol.*, vol. 22, no. 5, pp. 1813–1827, Sep. 2014.
- [7] C. A. Hans, V. Nenchev, J. Raisch, and C. Reincke-Collon, "Minimax model predictive operation control of microgrids," *IFAC Proceedings Volumes*, vol. 47, no. 3, pp. 10287–10292, 2014, 19th IFAC World Congress. [Online]. Available: <http://www.sciencedirect.com/science/article/pii/S1474667016432465>
- [8] M. B. Saltik, L. Özkan, J. H. A. Ludlage, S. Weiland, and P. M. J. Van den Hof, "An outlook on robust model predictive control algorithms: Reflections on performance and computational aspects," *Journal of Process Control*, vol. 61, pp. 77–102, 2018. [Online]. Available: <http://www.sciencedirect.com/science/article/pii/S0959152417301968>
- [9] J. Löfberg, "Minimax approaches to robust model predictive control," Ph.D. dissertation, Department of Electrical Engineering, Linköping University, Linköping, Sweden, 2003.
- [10] A. Bemporad, F. Borrelli, and M. Morari, "Min-max control of constrained uncertain discrete-time linear systems," *IEEE Transactions on Automatic Control*, vol. 48, no. 9, pp. 1600–1606, Sept 2003.
- [11] I. U. Nutkani, P. C. Loh, P. Wang, and F. Blaabjerg, "Cost-prioritized droop schemes for autonomous ac microgrids," *IEEE Transactions on Power Electronics*, vol. 30, no. 2, pp. 1109–1119, Feb 2015.
- [12] —, "Linear decentralized power sharing schemes for economic operation of ac microgrids," *IEEE Transactions on Industrial Electronics*, vol. 63, no. 1, pp. 225–234, Jan 2016.
- [13] F. Chen, M. Chen, Q. Li, K. Meng, Y. Zheng, J. M. Guerrero, and D. Abbott, "Cost-based droop schemes for economic dispatch in islanded microgrids," *IEEE Transactions on Smart Grid*, vol. 8, no. 1, pp. 63–74, Jan 2017.
- [14] F. Dörfler, J. W. Simpson-Porco, and F. Bullo, "Breaking the hierarchy: Distributed control and economic optimality in microgrids," *IEEE Transactions on Control of Network Systems*, vol. 3, no. 3, pp. 241–253, Sept 2016.
- [15] Y.-Y. Cao and Z. Lin, "Min-max mpc algorithm for lpv systems subject to input saturation," *IEE Proceedings - Control Theory and Applications*, vol. 152, no. 3, pp. 266–272, May 2005.
- [16] H. Huang, D. Li, Z. Lin, and Y. Xi, "An improved robust model predictive control design in the presence of actuator saturation," *Automatica*, vol. 47, no. 4, pp. 861–864, 2011. [Online]. Available: <http://www.sciencedirect.com/science/article/pii/S0005109811000604>
- [17] J. Oravec and M. Bakošová, "Robust model predictive control based on nominal system optimization and control input saturation," *IFAC-PapersOnLine*, vol. 48, no. 14, pp. 314–319, 2015, 8th IFAC Symposium on Robust Control Design ROCOND 2015. [Online]. Available: <http://www.sciencedirect.com/science/article/pii/S2405896315015955>
- [18] T. L. Vandoorn, J. D. Kooning, B. Meersman, and L. Vandevelde, "Voltage-based droop control of renewables to avoid on-off oscillations caused by overvoltages," *IEEE Transactions on Power Delivery*, vol. 28, no. 2, pp. 845–854, April 2013.
- [19] K. Das, M. Altin, A. D. Hansen, P. E. Sørensen, D. Flynn, and H. Abildgaard, "Wind power support during overfrequency emergency events," *CIGRE Science & Engineering*, vol. 9, pp. 73–83, 2018.
- [20] J. Neely, J. Johnson, J. Delhotal, S. Gonzalez, and M. Lave, "Evaluation of pv frequency-watt function for fast frequency reserves," in *2016 IEEE Applied Power Electronics Conference and Exposition (APEC)*, March 2016, pp. 1926–1933.
- [21] H. Xin, Y. Liu, Z. Wang, D. Gan, and T. Yang, "A new frequency regulation strategy for photovoltaic systems without energy storage," *IEEE Transactions on Sustainable Energy*, vol. 4, no. 4, pp. 985–993, Oct 2013.
- [22] J. Pauphilet, D. Kiner, D. Faille, and L. El Ghaoui, "A tractable numerical strategy for robust milp and application to energy management," in *2016 IEEE 55th Conference on Decision and Control (CDC)*, Dec 2016, pp. 1490–1495.
- [23] C. A. Hans, P. Sotasakis, J. Raisch, C. Reincke-Collon, and P. Patrinos, "Risk-averse model predictive operation control of islanded microgrids," *IEEE Transactions on Control Systems Technology*, vol. 28, no. 6, pp. 2136–2151, Nov. 2020. [Online]. Available: <https://ieeexplore.ieee.org/document/8792379>
- [24] A. Krishna, C. A. Hans, J. Schiffer, J. Raisch, and T. Kral, "Steady state evaluation of distributed secondary frequency control strategies for microgrids in the presence of clock drifts," in *2017 25th Mediterranean Conference on Control and Automation (MED)*, July 2017, pp. 508–515.
- [25] J. Schiffer, C. A. Hans, T. Kral, R. Ortega, and J. Raisch, "Modeling, analysis, and experimental validation of clock drift effects in low-inertia power systems," *IEEE Transactions on Industrial Electronics*, vol. 64, no. 7, pp. 5942–5951, July 2017.
- [26] R. J. Hyndman and G. Athanasopoulos, *Forecasting: principles and practice*. OTexts, 2018.
- [27] A. Bemporad and M. Morari, "Control of systems integrating logic, dynamics, and constraints," *Automatica*, vol. 35, no. 3, pp. 407–427, 1999. [Online]. Available: <http://www.sciencedirect.com/science/article/pii/S0005109898001782>
- [28] J. Löfberg, "YALMIP : a toolbox for modeling and optimization in MATLAB," in *2004 IEEE International Symposium on Computer Aided Control Systems Design*, Sept 2004, pp. 284–289.
- [29] Gurobi Optimization LLC, "Gurobi optimizer reference manual," 2018. [Online]. Available: <https://www.gurobi.com>
- [30] ARM, "Atmospheric Radiation Measurement Climate Research Facility, Surface Meteorology System (MET), Eastern North Atlantic Facility ARM Data Archive: Oak Ridge, USA," accessed July 14, 2011.
- [31] C. A. Hans and E. Klages, "Very short term time-series forecasting of solar irradiance without exogenous inputs," in *6th International Conference on Time Series and Forecasting (ITISE)*, 2019. [Online]. Available: <https://arxiv.org/abs/1810.07066>